The RND-family transporter, HpnN, is required for hopanoid localization to the outer membrane of *Rhodopseudomonas palustris* TIE-1

David M. Doughty[a,b], Maureen L. Coleman[a], Ryan C. Hunter[a,b], Alex L. Sessions[c], Roger E. Summons[d], and Dianne K. Newman[a,b,c,1]

[a]Division of Biology, [b]Howard Hughes Medical Institute, and [c]Division of Geological and Planetary Sciences, California Institute of Technology, Pasadena, CA 91125; and [d]Department of Earth, Atmospheric and Planetary Sciences, Massachusetts Institute of Technology, Cambridge, MA 02139

Edited by Thomas J. Silhavy, Princeton University, Princeton, NJ, and approved July 25, 2011 (received for review March 21, 2011)

Rhodopseudomonas palustris **TIE-1 is a Gram-negative bacterium that produces structurally diverse hopanoid lipids that are similar to eukaryotic steroids. Its genome encodes several homologues to proteins involved in eukaryotic steroid trafficking. In this study, we explored the possibility that two of these proteins are involved in intracellular hopanoid transport.** ***R. palustris*** **has a sophisticated membrane system comprising outer, cytoplasmic, and inner cytoplasmic membranes. It also divides asymmetrically, producing a mother and swarmer cell. We deleted genes encoding two putative hopanoid transporters that belong to the resistance–nodulation–cell division superfamily. Phenotypic analyses revealed that one of these putative transporters (HpnN) is essential for the movement of hopanoids from the cytoplasmic to the outer membrane, whereas the other (Rpal_4267) plays a minor role.** C_{30} **hopanoids, such as diploptene, are evenly distributed between mother and swarmer cells, whereas** ***hpnN*** **is required for the** C_{35} **hopanoid, bacteriohopanetetrol, to remain localized to the mother cell type. Mutant cells lacking HpnN grow like the WT at 30 °C but slower at 38 °C. Following cell division at 38 °C, the** Δ***hpnN*** **cells remain connected by their cell wall, forming long filaments. This phenotype may be attributed to hopanoid mislocalization because a double mutant deficient in both hopanoid biosynthesis and transport does not form filaments. However, the lack of hopanoids severely compromises cell growth at higher temperatures more generally. Because hopanoid mutants only manifest a strong phenotype under certain conditions,** ***R. palustris*** **is an attractive model organism in which to study their transport and function.**

bacteria | resistance–nodulation–cell division transporters | hopanols | microbial cell biology

Hopanoids are bacterial lipids that exhibit structural and biosynthetic similarity to eukaryotic steroids (Fig. 1*A*), with the exception that they can be synthesized under strictly anaerobic conditions whereas steroids cannot. Molecular fossils of steroids and hopanoids (steranes and hopanes, respectively) can be found in ancient sedimentary rocks that formed at least 2.7 billion years ago (1–3). Whereas steroids are well known to play important roles in eukaryotic membrane composition and curvature as well as intercellular signaling pathways (4–6), we know relatively little about the biological functions of hopanoids. Physiological studies have associated hopanoid production with changes in temperature, desiccation, pH, and cellular differentiation (7–11). The immense structural variation of hopanoids, including modification by methylation or the addition of diverse polar head groups (12, 13), suggests there may be specificity in their structures with regard to localization and/or function. Certain hopanoids, for instance, localize to the outer membrane of Gram-negative cells in the context of stress resistance (8), and other work has indicated that hopanoids are specifically found in the outer membrane of a variety of bacteria (8, 14, 15). However, the mechanism of intercellular hopanoid transport has not been explored.

Recently, an "unsolved mystery" featuring hopanoids was highlighted regarding the evolutionary history of proteins found in the Hedgehog signaling pathway (5). Hausmann et al. (5) argued that eukaryotic transporters [e.g. Patched, Dispatched, and the Niemann–Pick carrier protein 1 (NPC1)] involved in movement of cholesterol or cholesterol-modified morphogens likely arose from bacterial hopanoid transporters belonging to the resistance–nodulation–cell division (RND) superfamily. This hypothesis was based on sequence similarity between the eukaryotic proteins and a specific subfamily of bacterial RND transporters, termed HpnN, whose members are associated with hopanoid biosynthesis genes in bacterial genomes. The structural similarity between steroids and hopanoids—the putative substrates of these transporters—further supports this hypothesis. This model assumes that the HpnN subfamily plays a role in hopanoid transport, and predicts that the last common ancestor of the bacterial HpnN and eukaryotic transporters was also a hopanoid transporter.

To test this hypothesis, we chose to work with the Gram-negative bacterium *Rhodopseudomonas palustris* TIE-1, which has emerged in recent years as an attractive model organism in which to study hopanoid biology (10, 16–19). *R. palustris* can produce three different membrane types (outer, cytoplasmic, and inner cytoplasmic; these latter membranes are lamellar and are structurally reminiscent of the Golgi apparatus in eukaryotic cells) and also divides asymmetrically, producing distinct mother and swarmer cells. Its genome contains two putative RND transporters—Rpal_4254 (HpnN) and Rpal_4267—within the region of the *R. palustris* chromosome that encodes many of the hopanoid biosynthetic genes (Fig. 1*B*). By combining genetic and cell biological approaches, we identified one of these genes (*hpnN*) as being essential for hopanoid transport to the outer membrane. Here, we explore the evolutionary relationship of HpnN to steroid transporters, and demonstrate that it plays an important role in the growth of *R. palustris* at 38 °C.

Results

Phylogenetic Clues to the Function of Hopanoid-Associated RND Transporters. The RND superfamily is widespread across bacteria, archaea, and eukaryotes. The hopanoid-associated RND transporters Rpal_4254 and Rpal_4267 share characteristic topological features with this superfamily, namely 12 predicted

Author contributions: D.M.D., M.L.C., and D.K.N. designed research; D.M.D., M.L.C., and R.C.H. performed research; A.L.S. and R.E.S. contributed new reagents/analytic tools; D.M.D., M.L.C., A.L.S., R.E.S., and D.K.N. analyzed data; and D.M.D., M.L.C., and D.K.N. wrote the paper.

The authors declare no conflict of interest.

This article is a PNAS Direct Submission.

[1]To whom correspondence should be addressed. E-mail: dkn@caltech.edu.

See Author Summary on page 18207.

This article contains supporting information online at www.pnas.org/lookup/suppl/doi:10.1073/pnas.1104209108/-/DCSupplemental.

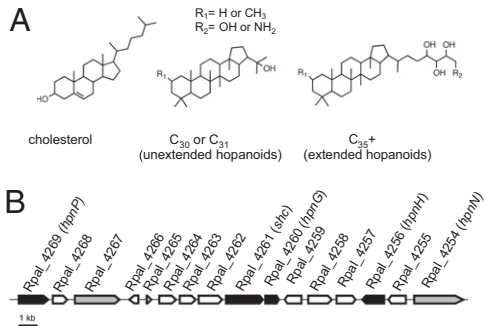

Fig. 1. Structures of cholesterol and hopanoid lipids and arrangement of hopanoid biosynthetic genes on the chromosome of *R. palustris* TIE-1. (*A*) Comparison of cholesterol and hopanoids. The "unextended" hopanoids (C_{30} or C_{31}) are generally considered to be intermediates in the biosynthesis of "extended" (C_{35}+) hopanoids. When R1 is H, the unextended hopanoid is called diplopterol. When R1 is H and R2 is OH, the extended hopanoid is called BHT (12). (*B*) Graphical depiction of the hopanoid biosynthetic gene cluster of *R. palustris* TIE-1 labeled by gene number and names. Genes known to be essential to hopanoid biosynthesis are shown in black, and genes encoding putative hopanoid transporters are shown in gray.

transmembrane helices with large extracytoplasmic loops between helices 1 and 2 and helices 7 and 8, as predicted by Krogh et al. (20). Unlike the well characterized tripartite efflux pumps of Gram-negative bacteria (e.g., AcrAB-TolC), the hopanoid-associated proteins appear to lack TolC docking domains and are not cotranscribed with a cognate adaptor protein. To gain insight into the function and evolutionary history of these proteins, we reconstructed their phylogeny relative to eight recognized families of RND transporters (Fig. 2). From the superfamily phylogeny, Rpal_4254 appears most closely related to family 8, whose sole characterized member is required for the accumulation of the pigment xanthomonadin in the outer membrane of *Xanthomonas oryzae* (21). Rpal_4267 is associated with family 7, whose members include archaeal and spirochete proteins of unknown function (22). Regardless of where the root is

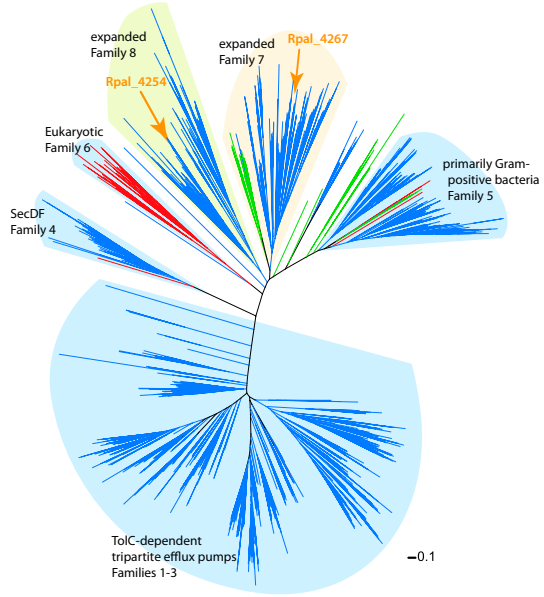

Fig. 2. Unrooted phylogeny of the RND superfamily showing the eight recognized families of RND transporters (www.tcdb.org) (22). The phylogenetic associations of Rpal_4254 and Rpal_4267 within these families are indicated by the arrows. (Scale bar: amino acid substitutions per site.)

placed in our RND superfamily phylogeny (Fig. 2), the eukaryotic family 6 transporters and the HpnN-containing family 8 cannot be sister clades, indicating that the eukaryotic Patched family of proteins (family 6) is no more closely related to HpnN than to other families of bacterial RND transporters (5).

To assess how widespread hopanoid-associated RND transporters might be beyond just *R. palustris*, a second phylogeny was constructed, this time focused on proteins from families 7 and 8 (Fig. 3 and Fig. S1). Because most proteins in these two families come from organisms lacking squalene-hopene cyclase (Fig. 3, inner ring), the potential for hopanoid intracellular transport is relatively restricted. To further support a function in hopanoid transport, we asked whether the RND-encoding gene was near hopanoid biosynthesis genes on the chromosome (Fig. 3, outer ring). Several good candidates for hopanoid transport emerged: the HpnN-like clade, which includes Rpal_4254 and is found in diverse proteobacteria; a smaller Rpal_4267-like clade confined to closely related α-proteobacteria; and a lone archaeal isolate, *Halorubrum lacusprofundi*. Because the HpnN-like clade contains a diversity of known hopanoid producing bacteria spanning α-, β-, γ-, and δ-proteobacteria, we hypothesized that it might be involved in the intracellular localization of hopanoids in *R. palustris* (Fig. 3).

Rpal_4254 (HpnN) Is Essential for Bacteriohopanetetrol Localization to Outer Membrane. Hopanoids were found to comprise 12.5 ± 1 μg × mg total lipid extract (TLE)$^{-1}$ of membrane fractions of *R. palustris* (Fig. 4). The most abundant hopanoid was bacteriohopanetetrol (BHT), which composed 8.1 ± 0.7 μg × mg TLE^{-1} of the whole cell (Fig. 4). The C_{30} hopanoids (e.g., diploptene; Fig. 1) were less abundant and collectively composed 3.8 ± 0.3 μg × mg TLE^{-1} and 8.7 ± 2.8 μg × mg TLE^{-1} of the whole cell and outer membrane fractions, respectively. Deletion of the genes encoding the two hopanoid associated RND transporters (Rpal_4254 and Rpal_4267) created mutant strains with different phenotypes. Whereas the Rpal_4254 mutant no longer contained any hopanoids in the outer membrane (Fig. 4), the Rpal_4267 mutant still contained a significant percentage (Fig. S2). Interestingly, the Rpal_4267 mutant produced more 2-methylhopanoids then observed in the WT or Rpal_4254 mutant, possibly indicating some role for Rpal_4267 in hopanoid homeostasis.

Because the Rpal_4267 mutant was only mildly compromised in hopanoid transport, we focused our characterization efforts on the Rpal_4254 mutant, which we refer to henceforth as *ΔhpnN*. *ΔhpnN* contained elevated concentrations of hopanoids in the cytoplasmic and inner cytoplasmic membrane fractions. For example, BHT increased from 4.4 ± 1.9 μg × mg TLE^{-1} in WT to 11.89 ± 2.0 μg × mg TLE^{-1} in *ΔhpnN* (Summary Figure). To verify that the loss of hopanoids in the outer membrane was a result of the deletion of *hpnN*, we performed a complementation experiment. When the *hpnN* gene was expressed on a multicopy plasmid in the *ΔhpnN* mutant background, hopanoid transport to the outer membrane was restored. Interestingly, whereas the whole-cell hopanoid composition of *ΔhpnN* did not change significantly relative to WT, complementation of the *ΔhpnN* mutant stimulated C_{30} hopanoid biosynthesis and transport to the outer membrane (Fig. 4); this is potentially a result of expression of *hpnN* from a multicopy plasmid.

Hopanoid Expression Is Correlated to Cell Cycle of *R. palustris*. The cell cycle of *R. palustris* is obligately bimodal with each cell division resulting in the production of a mother cell and a flagellated swarmer cell. Because these cell types have different biological functions and different membrane structures (e.g., mother cells produce buds from one end of the cell, which become swarmer cells), we decided to explore the expression of hopanoids in the context of the cell cycle. Synchronous cultures of *R. palustris* were created using the sucrose density gradient pro-

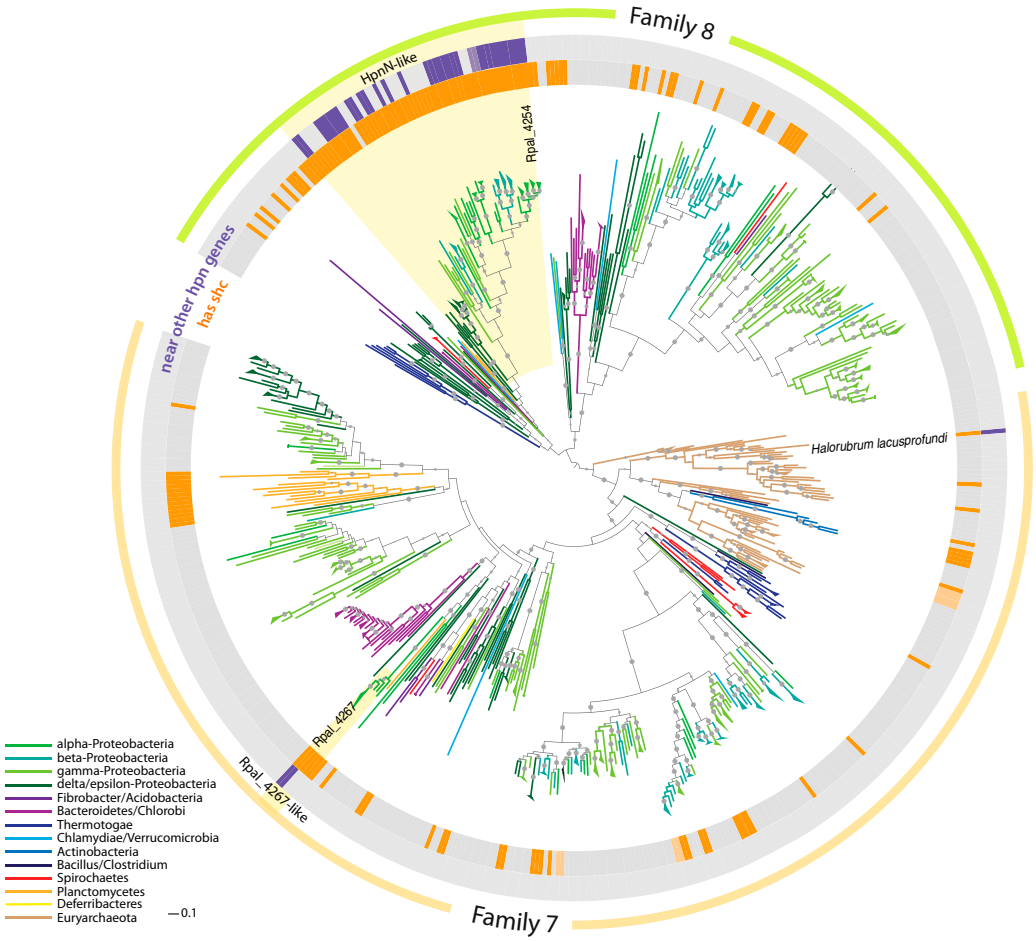

Fig. 3. Maximum likelihood phylogeny of two families of RND transporters associated with hopanoid transport. Concentric rings depict co-occurrence of squalene hopene cyclase in the genome (inner ring) and proximity to genes known to be involved in hopanoid biosynthesis (outer ring). Nodes with bootstrap support greater than 95% are marked with a gray circle. For clarity, sequence names have been omitted and closely related clades have been collapsed; the full version is shown in Fig. S1.

tocol described by Westmacott and Primrose (23). We followed the growth of swarmer cells into mother cells by light microscopy and observed the loss of motility (i.e., conversion to mother cell), the budding growth of the swarmer cell from the mother cell, followed by cell division (Fig. 5*A*). Cultures doubled in direct cell count between hours 5 and 6, suggesting growth had been successfully synchronized (Fig. 5*B*). The relative DNA content of cells was followed by using the PicoGreen dsDNA stain, and a doubling of DNA staining at hour 5 confirmed that more than 95% of the cells in the synchronized culture contained a second copy of the chromosome (Fig. 5*B*). At the start of our synchronized growth experiment, swarmer cells were devoid of BHT to the limit of detection of approximately 1 μg BHT × mg TLE^{-1} (Fig. 5*C*). In contrast, C_{30} hopanoids were found in equal amounts in mother and swarmer cells. This may imply that different hopanoids have different cellular functions. The hopanoid content of the synchronized cultures increased to 20 μg BHT × mg^{-1} TLE within 2 h of incubation in complete medium (Fig. 5*C*). BHT synthesized during the growth of swarmer cells into mother cells was exclusively produced in the desmethyl form. Following cell division, swarmer cells were separated from mother cells by density gradient centrifugation. The new population of swarmer cells contained trace amounts of BHT (possibly resulting from imperfect separation from mother cells) whereas the mother cells contained 20 μg BHT × mg^{-1} TLE. These data demonstrate that the synthesis of BHT is correlated to the cell cycle in *R. palustris*. Interestingly, both BHT and 2-methylBHT were detected in swarmer cells of *ΔhpnN* (Fig. S3). Because total hopanoid abundance was unchanged in *ΔhpnN*, the occurrence of BHT in swarmer cells is unlikely to result from up-regulation of hopanoid biosynthesis. Instead, diffusion of BHT and 2-methylBHT from the cytoplasmic membrane of mother cells to that of swarmer cells seems probable.

Permissive and Selective Growth of Mutant Strains in Response to Temperature. Separate from the question of whether hopanoid production is cell cycle-associated, we were interested in exploring whether specific environmental conditions might elicit their production. Because hopanoid production by other bacteria is stimulated at elevated growth temperatures (7, 11), we set out to determine whether this is also the case for *R. palustris*. When the growth temperature was increased from 30 °C to 38 °C, whole-cell BHT content increased by approximately 25%. Accordingly, we predicted that the growth of *ΔhpnN* would be conditionally sensitive to temperature. To test this hypothesis, two control strains were constructed: one that cannot produce hopanoids (*Δshc*) and one that neither produces hopanoids nor contains the *hpnN* gene (*ΔshcΔhpnN*). Increasing the temperature from 30 to 38 °C slightly increased the growth rate of the WT, but *ΔhpnN*, *Δshc*, and *ΔshcΔhpnN* all grew more slowly and to lower OD_{600} at 38 °C than at 30 °C (Fig. 6 *A* and *B*). The expression of *hpnN* from pDMD5 restored normal growth to the

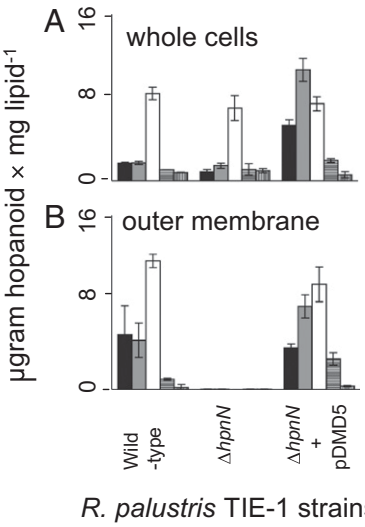

Fig. 4. Whole cell (*A*) and outer membrane (*B*) hopanoid content of WT, *ΔhpnN*, and *ΔhpnN* strain complemented with pDMD5. Hopanoids are diploptene (black), 2-methyldiploptene (gray), BHT (white), 2-methylBHT (horizontal stripes), and bacteriohopaneaminotriol (vertical stripes). The error bars represent the SD from the mean of three independent cultures.

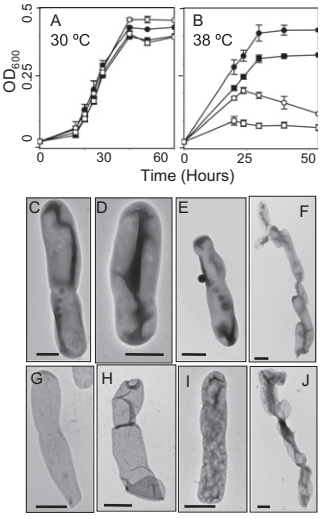

Fig. 6. The effects of elevated temperature on cell growth and physiology. Growth curves conducted at 30 °C (*A*) and 38 °C (*B*) on the WT (●), *ΔhpnN* (■), *Δshc* (○), and *ΔhpnNΔshc* (□). Error bars represent the SD from the means of three independent cultures. Visualization of whole cell morphology in WT grown at 30 °C (*C*) and 38 °C (*D*) and of *ΔhpnN* grown at 30 °C (*E*) and 38 °C (*F*). Visualization of peptidoglycan sacculi in WT grown at 30 °C (*G*) and 38 °C (*H*) and of *ΔhpnN* grown at 30 °C (*I*) and 38 °C (I). (Scale bars: *C–J*, 0.5 µm.)

ΔhpnN mutant compared with that of an empty vector control in the WT background; the empty vector control did not complement *ΔhpnN*. *ΔhpnN* was not as significantly affected as *Δshc*, suggesting that hopanoids can partially protect cells from elevated temperature when localized to the cytoplasmic and inner cytoplasmic membrane(s). Although we cannot rule out the possibility that the growth defect in the *Δshc* mutant is caused by the buildup of squalene, when succinate was supplied to stationary-phase cultures at 38 °C, it stimulated the growth of all strains. This, together with the fact that both the *Δshc* and *ΔhpnN* mutants appear to shed membrane material more than the WT,

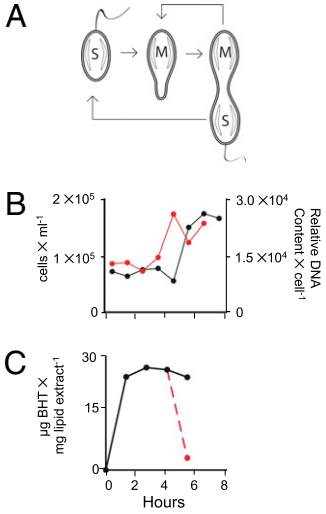

Fig. 5. Physiology and hopanoid production in synchronized cultures of *R. palustris*. (*A*) Physical depiction of the cell cycle of *R. palustris* TIE-1. (*B*) Direct cell count (black line) and DNA content (red line) of cells in a representative synchronized culture (four independent cultures were analyzed). (*C*) BHT content of a representative synchronized culture (three independent cultures were analyzed). The black line follows BHT concentration in a swarmer cell as it grows into a mother cell. The red line indicates the BHT concentration of the new swarmer cell that is formed following one cell cycle.

suggests that carbon limitation may underpin the growth defect as opposed to squalene being toxic per se. A growth handicap at 38 °C was most pronounced for *ΔshcΔhpnN*, suggesting that HpnN has additional roles besides transporting hopanoids.

Temperature-Dependent Cellular Filamentation Results from Hopanoid Mislocalization. We predicted that the slow growth and low yield of the hopanoid transport and/or biosynthesis mutant strains at elevated temperature might correlate with specific morphological deformities. To test this, we visualized the WT and mutants by light and transmission EM. *R. palustris* TIE-1 formed single cells at both 30 °C and 38 °C (Fig. 6 *C* and *D*), whereas mutant strains displayed diverse morphologies. *ΔhpnN* formed single cells when grown at 30 °C (Fig. 6*E*), yet filamented when grown at 38 °C (Fig. 6*F*); complementation of *ΔhpnN* with *hpnN* expressed on pDMD5 allowed the strain to divide normally at 38 °C, whereas an empty vector control did not. In contrast to *ΔhpnN*, *Δshc* and *ΔshcΔhpnN* formed single cells at both 30 °C and 38 °C but sometimes had small blebs localized to one pole at 38 °C (Fig. S4), suggesting that the observed temperature-dependent growth and morphological phenotypes may be caused by separate phenomena. Because the lack of filamentation in the *Δshc* and *ΔshcΔhpnN* mutants could have resulted from poor growth, we added 20 mM succinate to these cultures to stimulate their growth to an OD_{600} of 0.4, comparable to that of WT. Under these conditions, neither mutant filamented. This indicates that hopanoid mislocalization, rather than the absence of hopanoids in the outer membrane, is responsible for the filamentation phenotype observed at 38 °C. However, we cannot yet rule out the possibility that the growth rate, even in the presence of added succinate, was below that needed to trigger filamentation.

Relative DNA concentration was measured by flow cytometry to verify the chromosome was replicating in the filamented cells. When synchronous cultures of *ΔhpnN* were grown at 30 °C, the DNA content of the cell population doubled just before cell division (Fig. S5*A*). In contrast, when *ΔhpnN* was grown at 38 °C, the DNA content increased well above that seen for swarmer or predivisional cells at 30 °C (Fig. S5*B*), indicating that the 38 °C cells were replicating their chromosome. Interestingly, when

PicoGreen dsDNA dye was used to visualize DNA within the cells by fluorescence microscopy, fluorescence was typically confined to one end of the filament (Fig. S4 *C–E*). These results suggest that although chromosome replication had occurred, chromosome partitioning was impaired in the filament. Because cellular morphology often tracks with that of the cell wall, we tested whether there were differences in the peptidoglycan sacculi of the WT and *ΔhpnN* (Fig. 6 *G–J*). The sacculi of WT cells were consistent with their whole cells' dimensions, whereas the sacculi of filamented *ΔhpnN* cells were regularly constricted (Fig. 6*J*). These data indicate that cell division at the level of peptidoglycan synthesis or hydrolysis was detrimentally affected in *ΔhpnN* at 38 °C.

Discussion

In this study, we have shown that HpnN is required for hopanoid transport. Together with our phylogenetic analysis, our phenotypic data supports the hypothesis that eukaryotic cholesterol and lipidated-morphogen transporters are evolutionarily related to lipid-translocating bacterial RND transporters. However, we believe it is premature to conclude that the eukaryotic transporters arose specifically from a bacterial hopanoid transporter. Based on our phylogenies, this scenario would require that the families containing HpnN and the eukaryotic steroid transporters descended from a common hopanoid-transporting ancestor. Two issues complicate this scenario. First, the potential for hopanoid transport within the HpnN-containing family of the RND transporters—as judged by the ability of the bacteria with HpnN-like proteins to make hopanoids—is relatively limited, and indeed another member of the family has been shown to transport pigments instead (21). Thus, it is possible that the ancestor of this family transported a substrate other than hopanoids. Second, regardless of where the root is placed in our RND superfamily phylogeny (Fig. 2), the eukaryotic family 6 transporters and the HpnN-containing family 8 cannot be sister clades (24). This evolutionary complexity notwithstanding, both our functional and phylogenetic data support the use of bacterial model systems to gain insight into sterol trafficking in eukaryotes.

The asymmetric distribution of certain hopanoids between mother and daughter cells is intriguing, and given recent indications of subcellular lipid localization in bacteria (25, 26), it is tempting to speculate that hopanoids may segregate at an even smaller scale. By analogy to studies demonstrating cholesterol's role in generating protein–lipid microdomains with specific cellular functions (27), it is conceivable that asymmetric hopanoid distribution might promote cell division at elevated growth temperatures by participating in the formation of protein–lipid microdomains, resulting in the recruitment of cell division machinery to the proper subcellular region. Hopanoids might not be needed to organize such domains at lower temperatures because of a more rigid bacterial membrane in which protein organization might be more stable. Alternatively, hopanoids themselves might interact directly with cell division machinery, much as steroids have been shown to serve as allosteric affectors of other proteins (28). Related to this, it is noteworthy that the genome of *R. palustris* TIE-1 contains two putative sterol-binding proteins that also contain metallo-β-lactamase domains. Such domains are found in proteins that catalyze peptidoglycan hydrolysis (29). Interestingly, *Escherichia coli* outer membrane lipoproteins are known to activate cell wall polymerases (30, 31) and possibly also recruit peptidoglycan hydrolases at septal sites (31). By analogy, it is possible that hopanoids might play an analogous role in *R. palustris* under temperature stress, consistent with the irregular peptidoglycan sacculi observed during growth of *ΔhpnN* at 38 °C. However, as tantalizing as these scenarios might be, it is equally possible that hopanoids play no role in cell division, but rather, hopanoid mislocalization at 38 °C elicits a general stress response resulting in defective cell division. By the same token, hopanoids appear to play a key role in promoting growth at 38 °C more generally, but it is also possible that the accumulation of squalene is toxic under these conditions. We will attempt to distinguish between these options in future studies.

As previously mentioned, steroids are known to interact with other lipids and proteins in eukaryotic cells in specific and meaningful ways. For example, structural modifications of sterols can have a dramatic impact on their biological function in higher organisms as well as influencing membrane curvature (32). In this context, it is noteworthy that hopanoid expression peaks in mother cells as they bear swarmer cells, a time when dramatic changes in membrane curvature occur. Of relevance is the fact that eukaryotic RND transporters similar to HpnN have been shown to be important in facilitating tubulation in eukaryotic cells, presumably through lipid trafficking (33–35). For example, in the nematode *Caenorhabditis elegans*, the proper assembly of a tubular channel through which sensory neurons access the outside environment is controlled by the HpnN-like proteins DAF-6 and CHE-14 (35). Although the precise mechanism whereby these proteins affect tubulation is not understood, it is thought that they contribute to tuning the balance between exocytosis and endocytosis to permit vesicle coalescence and the generation of a tube through the cell (35). It is unclear if HpnN bears mechanistic similarity to the Daf6 protein, but given that the budding growth (i.e., tube) bridging *R. palustris* mother cells and swarmer cells is at a similar scale to the tubular channel in *C. elegans* (35), it is worth investigating whether hopanoids localize to this part of the predivisional cell body in an HpnN-dependent manner.

Unlike eukaryotic steroids, hopanoids and their transporters are not essential in *R. palustris* TIE-1 (10), providing us with the opportunity to study the functional consequence of hopanoid transport and localization in a living cell. In the years to come, it will be interesting to identify the similarities and differences between hopanoids and steroids with respect to their biophysical properties and cellular functions. Given that hopanoids are remarkably geo-stable, a better appreciation of their biological functions will improve our evolutionary interpretations of their ancient molecular fossils.

Methods

Phylogeny of HpnN. The phylogeny of the entire RND superfamily was inferred based on the transmembrane domains, which are more conserved than the extracytoplasmic loops. We identified 8,999 proteins containing two instances of the structural domain SCOP 82866 (multidrug efflux transporter AcrB transmembrane domain) in the MicrobesOnline public database (36). These domains were aligned by using HMMER3 (http://hmmer.org) to the profile HMM for SCOP 82866, and the tree was reconstructed using FastTree 2.1.3 (37). The resulting unrooted tree shown in Fig. 2 largely recovers the families defined by Tseng et al. (22). We then aligned full-length proteins from families 7 and 8 by using the most accurate mode (L-INS-i) in MAFFT, version 6.843b (38, 39), trimmed the alignment with Gblocks 0.91b (40), inferred maximum likelihood trees by using RAxML 7.0.4 (41), and visualized the tree by using iToL (42). Additional details are described in *SI Methods*.

Culture Conditions. Bacterial strains used in this study are listed in Table S1. Medium and culturing protocols for the growth of *R. palustris* and *E. coli* were conducted under photoheterotrophic growth conditions as described previously (17). Synchronized cultures of *R. palustris* were created using a sucrose density gradient to isolate swarmer cells, as described by Westmacott and Primrose (23).

DNA Methods, Plasmid Construction, and Transformation. All plasmids and primers used in this study are described in Table S2. The construction of clean deletion mutants of the Rpal_4254 and Rpal_4267 genes was carried out by the gentamicin selection, sucrose counter-selection method described previously (43). The generation of complementing plasmids was carried out as previously described (43).

Membrane Preparations of *R. palustris*. The outer membrane of *R. palustris* was removed by gentle sonication in a 20 mM 3-(N-morpholino)propanesulfonic acid (MOPS, pH 7.2) buffer and 5 mM EDTA. Cells were pelleted by centrifugation at 5,000 × *g* for 20 min at 4 °C, and the supernatant containing outer membrane was collected. Aliquots of the outer membrane containing supernatant were layered on top of a 40% sucrose solution and subjected to ultracentrifugation at 50,000 × *g* for 2 h at 4 °C. Following ultracentrifugation, the outer membrane formed a pellet at the bottom of the centrifuge tube and the cytoplasmic membrane remained in the supernatant. The presence of phytadiene isomers, the breakdown product of the pigment phytol, were identified based upon previously published spectra (44, 45), and served as a control to establish that the outer membrane fractions were not contaminated with cytoplasmic and inner cytoplasmic membrane lipid material (Fig. S6). The high concentrations of sucrose in the membrane fractionation interfered with the extraction of hopanoids from membranes and accurate assessment of dry weight. To overcome this obstacle, the outer membrane was washed to rid it of sucrose. Briefly, the outer membrane pellet was resuspended in 10 mM MOPS, pH 7, to its original volume and subjected to ultracentrifugation at 50,000 × *g* for 2 h at 4 °C. Cytoplasmic and inner cytoplasmic membrane fractions were prepared using similar methods as described in *SI Methods*.

Lipid Extractions and Hopanoid Quantification. Hopanoids were quantified by the high-temperature GC-MS protocols developed by Welander et al. (10, 17), except silica gel columns were used to distinguish variation in the abundances of hydrocarbon and alcohol structures. 2-Methylhopenes could not be detected in the hexane fraction from the silica gel columns (Fig. S6). These results suggest 2-methylhopenes are formed from 2-methyldipolpterol during some of the steps of the analytical protocol. In the present study, we do not distinguish between diplopterol and diploptenes; rather, we extended the incubation of lipid extracts with pyridine and acetic anhydride to 30 min at 70 °C, only diploptene and 2-methyldiploptene could be detected, and they were quantified as described previously (8). The extended hopanoids BHT, 2-methylBHT, and bacteriohopaneaminotriol were detected as described previously (10, 17).

EM. For transmission EM of whole cells, *R. palustris* cultures were diluted to a concentration of 1×10^7 cells·mL^{-1} by using sterile water. A drop of the diluted culture was placed on Parafilm and grids were floated on the surface for approximately 10 min. Grids were then stained by transferring them onto droplets of 2% (wt/vol) uranyl acetate (UA) (36) for 30 s. Grids were washed with deionized water and blotted dry. For the visualization of peptidoglycan sacculi, cultures were harvested by centrifugation 5,000 × *g* for 10 min, resuspended in 10% SDS, and boiled for 30 min. The SDS solution was allowed to cool and was then subjected to ultracentrifugation at 50,000 × *g* for 2 h. Following ultracentrifugation, sacculi formed a pellet at the bottom of the tube, and were resuspended in 10% SDS and boiled for another 30 min. Sacculi were again harvested by ultracentrifugation and resuspended in water. Staining and visualization was accomplished as described for the whole cells.

ACKNOWLEDGMENTS. The authors thank Dr. Arpita Bose for assistance with molecular techniques, Dr. Julie Maresca for help with phylogenetic profiling, Carolyn Colonero for technical assistance with the GC-MS analyses, and the anonymous reviewers for constructive feedback that improved our manuscript. This work was supported by the Howard Hughes Medical Institute (HHMI) and grants from the NASA exobiology program (to D.K.N. and R.E.S.). D.K.N. is an HHMI Investigator. R.E.S. is supported by the National Science Foundation Chemical Oceanography Program.

1. Brocks JJ, Buick R, Logan GA, Summons RE (2003) Composition and syngeneity of molecular fossils from the 2.78 to 2.45 billion-year-old Mount Bruce Subgroup, Pibara Craton, Western Australia. *Geochim Cosmochim Acta* 67:4289–4319.
2. Eigenbrode JL (2008) Fossil lipids for life-detection: A case study from the early earth record. *Space Sci Rev* 135:161–185.
3. Waldbauer JR, Sherman LS, Sumner DY, Summons RE (2009) Late Archean molecular fossils from the Transvaal Supergroup record the antiquity of microbial diversity and aerobiosis. *Precambrian Res* 169:28–47.
4. Eaton S (2008) Multiple roles for lipids in the Hedgehog signalling pathway. *Nat Rev Mol Cell Biol* 9:437–445.
5. Hausmann G, von Mering C, Basler K (2009) The hedgehog signaling pathway: Where did it come from? *PLoS Biol* 7:e1000146.
6. Ikonen E, Jansen M (2008) Cellular sterol trafficking and metabolism: Spotlight on structure. *Curr Opin Cell Biol* 20:371–377.
7. Schmidt A, Bringer-Meyer S, Poralla K, Sahm H (1986) Effects of alcohols and temperature on the hopanoid content of *Zymomonas mobilis*. *Appl Microbiol Biotechnol* 25:32–36.
8. Doughty DM, Hunter RC, Summons RE, Newman DK (2009) 2-Methylhopanoids are maximally produced in akinetes of *Nostoc punctiforme*: geobiological implications. *Geobiology* 7:524–532.
9. Poralla K, Muth G, Härtner T (2000) Hopanoids are formed during transition from substrate to aerial hyphae in *Streptomyces coelicolor* A3(2). *FEMS Microbiol Lett* 189: 93–95.
10. Welander PV, et al. (2009) Hopanoids play a role in membrane integrity and pH homeostasis in *Rhodopseudomonas palustris* TIE-1. *J Bacteriol* 191:6145–6156.
11. Joyeux C, Fouchard S, Llopiz P, Neunlist S (2004) Influence of the temperature and the growth phase on the hopanoids and fatty acids content of *Frateuria aurantia* (DSMZ 6220). *FEMS Microbiol Ecol* 47:371–379.
12. Bradley AS, Pearson A, Saenz JP, Marx CJ (2010) Adenosylhopane: The first intermediate in hopanoid side chain biosynthesis. *Org Geochem* 41:1075–1081.
13. Talbot HM, Rohmer M, Farrimond P (2007) Structural characterisation of unsaturated bacterial hopanoids by atmospheric pressure chemical ionisation liquid chromatography/ion trap mass spectrometry. *Rapid Commun Mass Spectrom* 21:1613–1622.
14. Jürgens UJ, Simonin P, Rohmer M (1992) Localization and distribution of hopanoids in membrane systems of the cyanobacterium *Synechocystis* PCC 6714. *FEMS Microbiol Lett* 71:285–288.
15. Jahnke LL, Summons RE, Hope JM, Des Marais DJ (1999) Carbon isotopic fractionation in lipids from methanotrophic bacteria II: The effects of physiology and environmental parameters on the biosynthesis and isotopic signatures of biomarkers. *Geochim Cosmochim Acta* 63:79–93.
16. Neunlist S, Bisseret P, Rohmer M (1988) The hopanoids of the purple non-sulfur bacteria *Rhodopseudomonas palustris* and *Rhodopseudomonas acidophila* and the absolute configuration of bacteriohopanetetrol. *Eur J Biochem* 171:245–252.
17. Welander PV, Coleman ML, Sessions AL, Summons RE, Newman DK (2010) Identification of a methylase required for 2-methylhopanoid production and implications for the interpretation of sedimentary hopanes. *Proc Natl Acad Sci USA* 107:8537–8542.
18. Rashby SE, Sessions AL, Summons RE, Newman DK (2007) Biosynthesis of 2-methylbacteriohopanepolyols by an anoxygenic phototroph. *Proc Natl Acad Sci USA* 104:15099–15104.
19. Kleemann G, Kellner R, Poralla K (1994) Purification and properties of the squalene-hopene cyclase from *Rhodopseudomonas palustris*, a purple non-sulfur bacterium producing hopanoids and tetrahymanol. *Biochim Biophys Acta* 1210:317–320.
20. Krogh A, Larsson B, von Heijne G, Sonnhammer ELL (2001) Predicting transmembrane protein topology with a hidden Markov model: Application to complete genomes. *J Mol Biol* 305:567–580.
21. Goel AK, Rajagopal L, Nagesh N, Sonti RV (2002) Genetic locus encoding functions involved in biosynthesis and outer membrane localization of xanthomonadin in *Xanthomonas oryzae pv. oryzae*. *J Bacteriol* 184:3539–3548.
22. Tseng TT, et al. (1999) The RND permease superfamily: An ancient, ubiquitous and diverse family that includes human disease and development proteins. *J Mol Microbiol Biotechnol* 1:107–125.
23. Westmacott D, Primrose SB (1976) Synchronous growth of *Rhodopseudomonas palustris* from the swarmer phase. *J Gen Microbiol* 94:117–125.
24. Lapointe FJ, Lopez P, Boucher Y, Koenig J, Bapteste E (2010) Clanistics: A multi-level perspective for harvesting unrooted gene trees. *Trends Microbiol* 18:341–347.
25. López D, Kolter R (2010) Functional microdomains in bacterial membranes. *Genes Dev* 24:1893–1902.
26. Renner LD, Weibel DB (2011) Cardiolipin microdomains localize to negatively curved regions of *Escherichia coli* membranes. *Proc Natl Acad Sci USA* 108:6264–6269.
27. Lingwood D, Simons K (2010) Lipid rafts as a membrane-organizing principle. *Science* 327:46–50.
28. Li X, Gianoulis TA, Yip KY, Gerstein M, Snyder M (2010) Extensive in vivo metabolite-protein interactions revealed by large-scale systematic analyses. *Cell* 143:639–650.
29. Firczuk M, Bochtler M (2007) Folds and activities of peptidoglycan amidases. *FEMS Microbiol Rev* 31:676–691.
30. Paradis-Bleau C, et al. (2010) Lipoprotein cofactors located in the outer membrane activate bacterial cell wall polymerases. *Cell* 143:1110–1120.
31. Typas A, et al. (2010) Regulation of peptidoglycan synthesis by outer-membrane proteins. *Cell* 143:1097–1109.
32. Bacia K, Schwille P, Kurzchalia T (2005) Sterol structure determines the separation of phases and the curvature of the liquid-ordered phase in model membranes. *Proc Natl Acad Sci USA* 102:3272–3277.
33. Zhang M, et al. (2001) Cessation of rapid late endosomal tubulovesicular trafficking in Niemann-Pick type C1 disease. *Proc Natl Acad Sci USA* 98:4466–4471.
34. Incardona JP (2005) From sensing cellular sterols to assembling sensory structures. *Dev Cell* 8:798–799.
35. Perens EA, Shaham S (2005) *C. elegans* daf-6 encodes a patched-related protein required for lumen formation. *Dev Cell* 8:893–906.
36. Dehal PS, et al. (2010) MicrobesOnline: an integrated portal for comparative and functional genomics. *Nucleic Acids Res* 38(database issue):D396–D400.
37. Price MN, Dehal PS, Arkin AP (2010) FastTree 2—approximately maximum-likelihood trees for large alignments. *PLoS ONE* 5:e9490.
38. Katoh K, Toh H (2008) Recent developments in the MAFFT multiple sequence alignment program. *Brief Bioinform* 9:286–298.

39. Nuin PA, Wang Z, Tillier ER (2006) The accuracy of several multiple sequence alignment programs for proteins. *BMC Bioinformatics* 7:471.
40. Talavera G, Castresana J (2007) Improvement of phylogenies after removing divergent and ambiguously aligned blocks from protein sequence alignments. *Syst Biol* 56:564–577.
41. Stamatakis A (2006) RAxML-VI-HPC: Maximum likelihood-based phylogenetic analyses with thousands of taxa and mixed models. *Bioinformatics* 22:2688–2690.
42. Letunic I, Bork P (2007) Interactive Tree Of Life (iTOL): An online tool for phylogenetic tree display and annotation. *Bioinformatics* 23:127–128.
43. Jiao Y, Kappler A, Croal LR, Newman DK (2005) Isolation and characterization of a genetically tractable photoautotrophic Fe(II)-oxidizing bacterium, *Rhodopseudomonas palustris* strain TIE-1. *Appl Environ Microbiol* 71:4487–4496.
44. Spooner N, et al. (1994) Stable carbon isotopic correlation of individual biolipids in aquatic organisms and a lake bottom sediment. *Org Geochem* 21:823–827.
45. Blumer M, Thomas DW (1965) Phytadienes in Zooplankton. *Science* 147:1148–1149.